

Evidence for κ Meson Production in

$J/\psi \rightarrow \bar{K}^*(892)^0 K^+ \pi^-$ Process

M. Ablikim¹, J. Z. Bai¹, Y. Ban¹⁵, J. G. Bian¹, X. Cai¹, H. F. Chen²¹,
H. S. Chen¹, H. X. Chen¹, J. C. Chen¹, Jin Chen¹, Y. B. Chen¹, S. P. Chi²,
Y. P. Chu¹, X. Z. Cui¹, Y. S. Dai²³, Z. Y. Deng¹, Q. F. Dong¹⁹, S. X. Du¹,
Z. Z. Du¹, J. Fang¹, S. S. Fang², C. D. Fu¹, C. S. Gao¹, Y. N. Gao¹⁹, S. D. Gu¹,
Y. T. Gu⁴, Y. N. Guo¹, Y. Q. Guo¹, Z. J. Guo²⁰, F. A. Harris²⁰, K. L. He¹,
M. He¹⁶, Y. K. Heng¹, H. M. Hu¹, T. Hu¹, G. S. Huang^{1a}, X. P. Huang¹,
X. T. Huang¹⁶, M. Ishida¹⁰, S. Ishida¹⁴, X. B. Ji¹, X. S. Jiang¹, J. B. Jiao¹⁶,
D. P. Jin¹, S. Jin¹, Yi Jin¹, T. Komada¹⁴, S. Kurokawa⁸, Y. F. Lai¹, G. Li²,
H. B. Li¹, H. H. Li¹, J. Li¹, R. Y. Li¹, S. M. Li¹, W. D. Li¹, W. G. Li¹, X. L. Li⁹,
X. Q. Li¹³, Y. L. Li⁴, Y. F. Liang¹⁷, H. B. Liao⁶, C. X. Liu¹, F. Liu⁶, Fang Liu²¹,
H. H. Liu¹, H. M. Liu¹, J. Liu¹⁵, J. B. Liu¹, J. P. Liu²², R. G. Liu¹, Z. A. Liu¹,
F. Lu¹, G. R. Lu⁵, H. J. Lu²¹, J. G. Lu¹, C. L. Luo¹², F. C. Ma⁹, H. L. Ma¹,
L. L. Ma¹, Q. M. Ma¹, X. B. Ma⁵, Z. P. Mao¹, T. Matsuda¹¹, X. H. Mo¹, J. Nie¹,
H. P. Peng²¹, N. D. Qi¹, H. Qin¹², J. F. Qiu¹, Z. Y. Ren¹, G. Rong¹, L. Y. Shan¹,
L. Shang¹, D. L. Shen¹, X. Y. Shen¹, H. Y. Sheng¹, F. Shi¹, X. Shi^{15b}, H. S. Sun¹,
J. F. Sun¹, S. S. Sun¹, Y. Z. Sun¹, Z. J. Sun¹, K. Takamatsu⁸, Z. Q. Tan⁴,
X. Tang¹, Y. R. Tian¹⁹, G. L. Tong¹, T. Tsuru⁸, K. Ukai⁸, D. Y. Wang¹,
L. Wang¹, L. S. Wang¹, M. Wang¹, P. Wang¹, P. L. Wang¹, W. F. Wang^{1c},
Y. F. Wang¹, Z. Wang¹, Z. Y. Wang¹, Zhe Wang¹, Zheng Wang², C. L. Wei¹,
D. H. Wei¹, N. Wu¹, X. M. Xia¹, X. X. Xie¹, B. Xin^{9a}, G. F. Xu¹, Y. Xu¹³,
K. Yamada¹⁴, I. Yamauchi¹⁸, M. L. Yan²¹, F. Yang¹³, H. X. Yang¹, J. Yang²¹,
Y. X. Yang³, M. H. Ye², Y. X. Ye²¹, Z. Y. Yi¹, G. W. Yu¹, J. M. Yuan¹,
Y. Yuan¹, S. L. Zang¹, Y. Zeng⁷, Yu Zeng¹, B. X. Zhang¹, B. Y. Zhang¹,
C. C. Zhang¹, D. H. Zhang¹, H. Y. Zhang¹, J. W. Zhang¹, J. Y. Zhang¹,
Q. J. Zhang¹, X. M. Zhang¹, X. Y. Zhang¹⁶, Yiyun Zhang¹⁷, Z. P. Zhang²¹,
Z. Q. Zhang⁵, D. X. Zhao¹, J. W. Zhao¹, M. G. Zhao¹³, P. P. Zhao¹, W. R. Zhao¹,
Z. G. Zhao^{1d}, H. Q. Zheng¹⁵, J. P. Zheng¹, Z. P. Zheng¹, L. Zhou¹, N. F. Zhou¹,
K. J. Zhu¹, Q. M. Zhu¹, Y. C. Zhu¹, Y. S. Zhu¹, Yingchun Zhu^{1e}, Z. A. Zhu¹,
B. A. Zhuang¹, X. A. Zhuang¹.

(BES Collaboration)

¹ *Institute of High Energy Physics, Beijing 100049, People's Republic of China*

² *China Center for Advanced Science and Technology (CCAST), Beijing 100080, People's Republic of China*

³ *Guangxi Normal University, Guilin 541004, People's Republic of China*

⁴ *Guangxi University, Nanning 530004, People's Republic of China*

⁵ *Henan Normal University, Xinxiang 453002, People's Republic of China*

⁶ *Huazhong Normal University, Wuhan 430079, People's Republic of China*

⁷ *Hunan University, Changsha 410082, People's Republic of China*

⁸ *KEK, High Energy Accelerator Research Organization, Ibaraki 305-0801, Japan*

⁹ *Liaoning University, Shenyang 110036, People's Republic of China*

¹⁰ *Meisei University, Tokyo 191-8506, Japan*

- ¹¹ *Miyazaki University, Miyazaki 889-2192, Japan*
- ¹² *Nanjing Normal University, Nanjing 210097, People's Republic of China*
- ¹³ *Nankai University, Tianjin 300071, People's Republic of China*
- ¹⁴ *Nihon University, Chiba 274-8501, Japan*
- ¹⁵ *Peking University, Beijing 100871, People's Republic of China*
- ¹⁶ *Shandong University, Jinan 250100, People's Republic of China*
- ¹⁷ *Sichuan University, Chengdu 610064, People's Republic of China*
- ¹⁸ *Tokyo Metropolitan College of Technology, Tokyo 140-0011, Japan*
- ¹⁹ *Tsinghua University, Beijing 100084, People's Republic of China*
- ²⁰ *University of Hawaii, Honolulu, HI 96822, USA*
- ²¹ *University of Science and Technology of China, Hefei 230026, People's Republic of China*
- ²² *Wuhan University, Wuhan 430072, People's Republic of China*
- ²³ *Zhejiang University, Hangzhou 310028, People's Republic of China*
- ^a *Current address: Purdue University, West Lafayette, IN 47907, USA*
- ^b *Current address: Cornell University, Ithaca, NY 14853, USA*
- ^c *Current address: Laboratoire de l'Accélérateur Linéaire, Orsay, F-91898, France*
- ^d *Current address: University of Michigan, Ann Arbor, MI 48109, USA*
- ^e *Current address: DESY, D-22607, Hamburg, Germany*

Abstract

Based on 58 million BESII J/ψ events, the $\bar{K}^*(892)^0 K^+ \pi^-$ channel in $K^+ K^- \pi^+ \pi^-$ is studied. A clear low mass enhancement in the invariant mass spectrum of $K^+ \pi^-$ is observed. The low mass enhancement does not come from background of other J/ψ decay channels, nor from phase space. Two independent partial wave analyses have been performed. Both analyses favor that the low mass enhancement is the κ , an isospinor scalar resonant state. The average mass and width of the κ in the two analyses are $878 \pm 23_{-55}^{+64}$ MeV/ c^2 and $499 \pm 52_{-87}^{+55}$ MeV/ c^2 , respectively, corresponding to a pole at $(841 \pm 30_{-73}^{+81}) - i(309 \pm 45_{-72}^{+48})$ MeV/ c^2 .

Key words: κ , low mass scalar, J/ψ decays, $K^*(892)^0 K \pi$

PACS: 13.25.Gv, 14.40.Ev

In the field of hadron spectroscopy, whether the low mass iso-scalar scalar meson, the σ , exists or not had been an important but controversial problem for many years. Recently, its evidence has been reported [1]-[5] not only in $\pi\pi$ scattering, but also in various production processes. The σ meson with a mass around 600 MeV/ c^2 and a broad width around 500 MeV/ c^2 is, now, widely accepted [6].

The evidence for the σ meson suggests the possibility of a σ nonet, $\{\sigma(600), \kappa(900), f_0(980), a_0(980)\}$, either in an extended linear sigma model realizing

chiral symmetry [7][8] or in a unitarized meson model [9]. The κ has been observed in analyses on $K\pi$ scattering phase shifts [10] by several groups using a unitarized meson method [9], an interfering amplitude method [11] considering a repulsive background suggested by chiral symmetry, and a nonperturbative method [12]-[14] with an effective chiral Lagrangian. The observed mass and width values are scattered in the ranges from 700 to 900 MeV/ c^2 and 550 to 650 MeV/ c^2 , respectively, depending on the model used. Recently, a rather wider width around 800 MeV/ c^2 was reported [15] for the κ in the analysis of $K\pi$ scattering phase shifts with a T-matrix method including a prescription for zero suppression. Also recently, an analysis of LASS data on πK scattering phase shifts using a unitarization method combined with chiral symmetry has found the κ with a slightly lighter pole mass [16]. However, some authors have found no evidence for the κ [17]-[19]. A criticism [20] has been presented for the existence of the κ based on unitarity and universality arguments, similar to the case of the σ [21][22].

Here, it is to be noted that in $\pi\pi$ and $K\pi$ scattering, effects due to σ and κ production are, as a result of chiral symmetry, largely cancelled by those due to non-resonant background scattering, while the cancellation mechanism does not necessarily work in the production process [23]. Therefore, it is more suitable for the investigation of σ/κ mesons to use the $\pi\pi/K\pi$ production process, which is parameterized independently of the scattering process [24].

Evidence for the κ has been reported, recently, in the production process by the E791 experiment at Fermilab in the analysis of $D^+ \rightarrow K^-\pi^+\pi^-$ [25]. Preliminary κ results have been reported [26] in the analysis of the $K\pi$ system produced in $J/\psi \rightarrow \bar{K}^*(892)^0 K^+\pi^-$ with BESII data. The FOCUS experiment has presented [27] evidence for the existence of a coherent $K\pi$ S-wave contribution to $D^+ \rightarrow K^-\pi^+\mu^+\nu$. CLEO [28] has seen no evidence for the κ in $D^0 \rightarrow K^-\pi^+\pi^0$. Preliminary results on the κ have also been reported in analyses of BESII data [29]-[31].

Here we report analyses of $\bar{K}^*(892)^0 K^+\pi^-$ in $J/\psi \rightarrow K^+K^-\pi^+\pi^-$ to study the κ . Partial wave analyses (PWA analyses) have been performed in $J/\psi \rightarrow \bar{K}^*(892)^0 K^+\pi^-$ using 58 million J/ψ decays obtained with BESII at the BEPC (Beijing Electron Positron Collider) storage ring. The BESII detector is described in detail elsewhere [32].

In the event selection, four charged tracks with zero net charge are required for each event. Every charged track should have a good helix fit in the Main Drift Chamber (MDC), and the polar angle θ of each track in the MDC must satisfy $|\cos\theta| < 0.8$. The event must originate near the collision point; tracks must satisfy $\sqrt{x^2 + y^2} \leq 2$ cm, $|z| \leq 20$ cm, where x , y and z are space coordinates of the point of closest approach of tracks to the beam axis. Particle

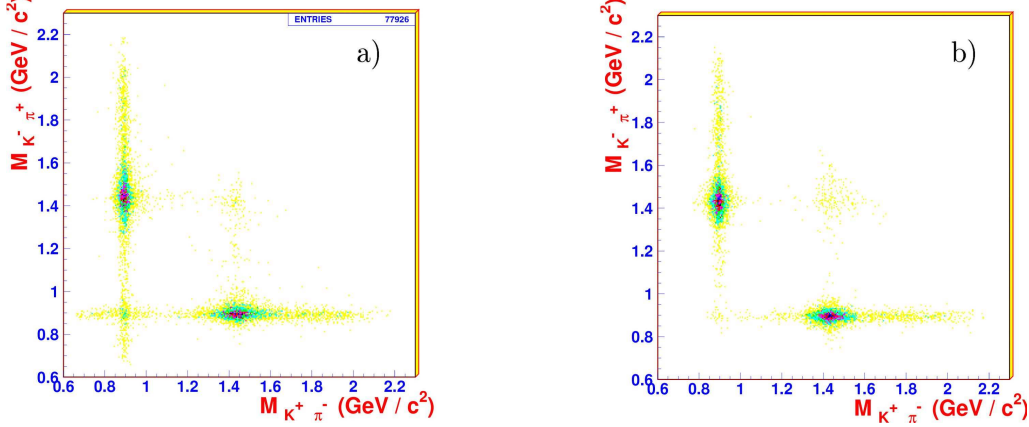


Fig. 1. a) Scatter plot of $M_{K^+\pi^-}$ versus $M_{K^-\pi^+}$ for BESII data. b) Scatter plot of $M_{K^+\pi^-}$ versus $M_{K^-\pi^+}$ for Monte Carlo simulation of $J/\psi \rightarrow \text{anything}$.

identification is performed using combined TOF and dE/dx information, and two identified kaons and two identified pions are required.

For a neutral track, it is required that it should have hits in the Barrel Shower Counter (BSC), the number of layers hit should be greater than one, the shower starts before layer 6, and its deposited energy is more than 50 MeV. The angle between the photon emission direction and the shower development direction of the track in the BSC should be less than 30° . An event associated with a neutral track(s) is rejected.

Surviving events are fitted kinematically (4C kinematic fits) under the hypotheses $J/\psi \rightarrow K^+K^-\pi^+\pi^-$, $\pi^+\pi^-\pi^+\pi^-$, $K^+K^-K^+K^-$, $K^+\pi^-\pi^+\pi^-$, and $\pi^+K^-\pi^+\pi^-$. It is required that $\chi_{4C}^2(K^+K^-\pi^+\pi^-)$ be less than 40. The sum of χ^2 of the 4C kinematic fit, TOF, and dE/dx for $K^+K^-\pi^+\pi^-$ is required to be less than those for the $\pi^+\pi^-\pi^+\pi^-$, $K^+K^-K^+K^-$, $K^+\pi^-\pi^+\pi^-$, and $\pi^+K^-\pi^+\pi^-$ hypotheses.

In order to remove background from $J/\psi \rightarrow \phi\pi^+\pi^-$, events with $|M_{K^+K^-} - 1.02| < 0.02$ GeV/ c^2 are vetoed, and to remove $J/\psi \rightarrow \bar{K}^*(892)^0 K_S^0$ background, events with $|M_{\pi^+\pi^-} - 0.497| < 0.04$ GeV/ c^2 and $R_{xy} > 0.8$ cm are vetoed, where $M_{K^+K^-}$ and $M_{\pi^+\pi^-}$ are the invariant masses of K^+K^- and $\pi^+\pi^-$, and R_{xy} is the decay length of K_S transverse to the beam axis.

Fig. 1a shows the scatter plot of $M_{K^+\pi^-}$ versus $M_{K^-\pi^+}$ after all above requirements. Two bands of $\bar{K}^*(892)^0$ and $K^*(892)^0$ corresponding to $J/\psi \rightarrow \bar{K}^*(892)^0 K^+\pi^-$ and $J/\psi \rightarrow K^*(892)^0 K^-\pi^+$, respectively, are clearly seen. There is an accumulation of events in the region where the two bands cross, which is not seen in the scatter plot of Monte Carlo $J/\psi \rightarrow \text{anything}$ events (shown in Fig. 1b) obtained with the Lund-charm generator [33], which is described below. This accumulation comes from J/ψ decaying to $\bar{K}^*(892)^0$ (or $K^*(892)^0$) against a low mass enhancement. The invariant mass spec-

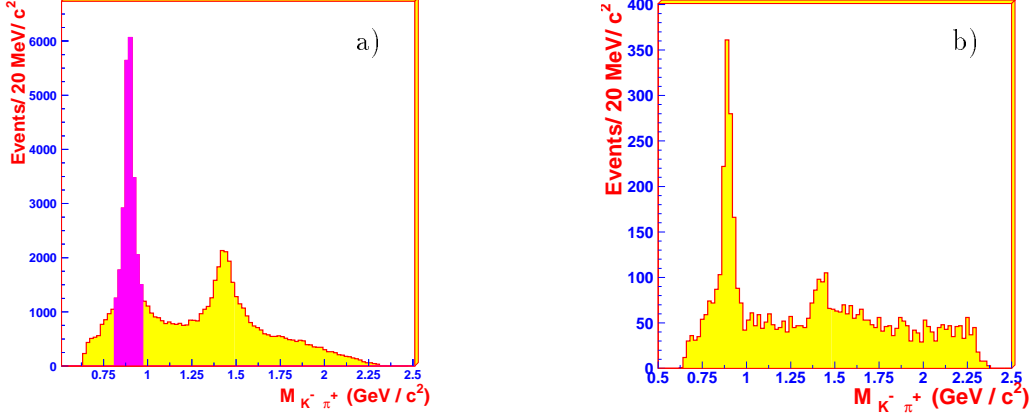


Fig. 2. a) Invariant mass spectrum for $K^-\pi^+$ after the final selection except the $\bar{K}^*(892)^0$ requirement. Events in the dark shaded area correspond to the data set in the present analyses. b) Recoil $K^-\pi^+$ mass distribution against the low mass enhancement ($M_{K^+\pi^-} < 0.8 \text{ GeV}/c^2$).

trum of $K^-\pi^+$ is shown in Fig. 2a, where the $\bar{K}^*(892)^0$ peak is clearly seen. The requirement $0.812 \text{ GeV}/c^2 < M_{K^-\pi^+} < 0.972 \text{ GeV}/c^2$ is imposed on the $J/\psi \rightarrow K^+K^-\pi^+\pi^-$ sample to select $J/\psi \rightarrow \bar{K}^*(892)^0K^+\pi^-$ events, the total number of which is 24674. The PWA analyses are applied to the selected $J/\psi \rightarrow \bar{K}^*(892)^0K^+\pi^-$ sample.

After the $\bar{K}^*(892)^0$ mass requirement, the $K^+\pi^-$ invariant mass distribution, shown as the solid histogram in Fig. 3a, has a clear $K^*(892)^0$ peak, a peak around $1430 \text{ MeV}/c^2$, and a broad enhancement in the low mass region. The $K^-\pi^+$ mass distribution of the charge conjugate channel $J/\psi \rightarrow K^*(892)^0K^-\pi^+$, denoted as crosses in Fig. 3a, shows the same structures.

Fig. 3c is the Dalitz plot of $J/\psi \rightarrow \bar{K}^*(892)^0K^+\pi^-$, and the insertion is that of its charge conjugate channel. In the Dalitz plot, the two diagonal bands correspond to the low mass enhancement and the peak around $1430 \text{ MeV}/c^2$ in the $K^+\pi^-$ invariant mass spectrum, and the horizontal band corresponds to $J/\psi \rightarrow K_1(1400)K$ and $K_1(1270)K$ with $K_1(1400)$ and $K_1(1270)$ decaying to $\bar{K}^*(892)^0\pi^-$. The clear top diagonal band in the Dalitz plot indicates that the low mass enhancement observed in this decay does not come from phase space since phase space events would be uniformly distributed in the Dalitz plot.

Though this low mass enhancement overlaps with the narrow $K^*(892)^0$, it can be clearly seen due to its broad structure. The spectrum of $K^-\pi^+$ mass recoiling against the low mass enhancement ($M_{K^+\pi^-} < 0.8 \text{ GeV}/c^2$) is shown in Fig. 2b, where a clear $\bar{K}^*(892)^0$ peak can be seen. This means that the low mass enhancement is produced dominantly through J/ψ decays associated with the $\bar{K}^*(892)^0$.

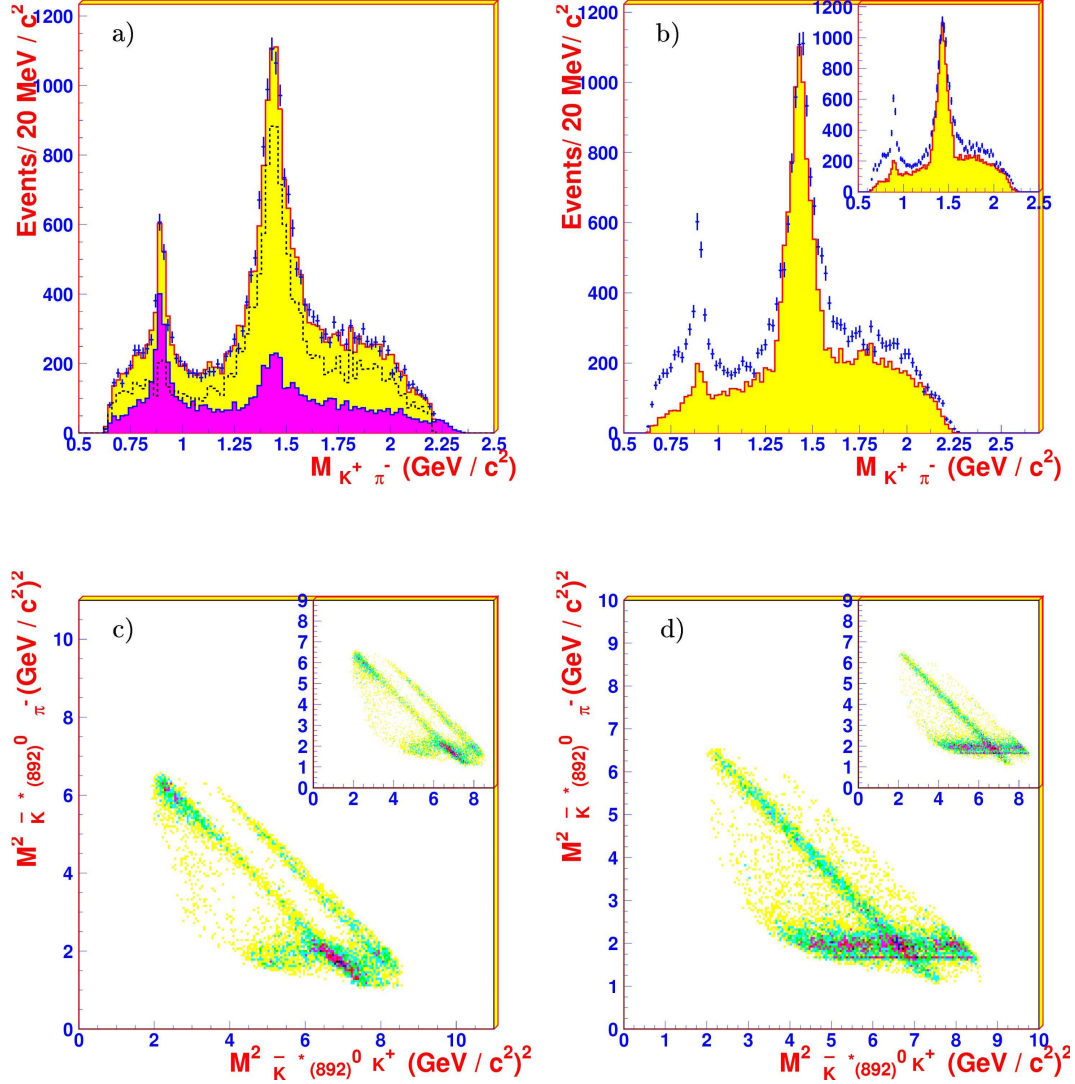


Fig. 3. a) Invariant mass spectrum of $K^+\pi^-$. The solid histogram is the data after the final selection, the dark shaded histogram is the $\bar{K}^*(892)^0$ side-band spectrum, and the dotted histogram is the invariant mass spectrum after side-band subtraction. Crosses with error bars show the charge conjugate state $K^-\pi^+$ from $J/\psi \rightarrow K^*(892)^0 K^-\pi^+$. b) Monte Carlo simulation compared with data. Crosses with error bars are data, and the solid histogram is Monte Carlo simulation. c) Dalitz plot of data, and d) that of Monte Carlo simulation. Those of the charge conjugate state are shown as inserts in b), c), and d).

$K^*(892)^0$ signals are clearly recognized in the $K^+\pi^-$ spectrum against $\bar{K}^*(892)^0$ side-band events (the dark shaded histogram) in Fig. 3a. The side-band events are taken from the $K^-\pi^+$ mass ranges directly neighboring to $\bar{K}^*(892)^0$ with 80 MeV/ c^2 widths. After side-band subtraction, the $K^*(892)^0$ peak is suppressed appreciably in the invariant mass spectrum of $K^+\pi^-$, as is shown in the same figure (the dotted histogram). This means that the $K^*(892)^0$ peak mostly comes from background processes. The main part of the broad low mass enhancement remains after side-band subtraction, which indicates that

the broad low mass structure does not come from J/ψ decay processes which do not contain $\bar{K}^*(892)^0$ in the final states.

The main background channels for $J/\psi \rightarrow \bar{K}^*(892)^0 K^+ \pi^-$ are studied through Monte Carlo simulation. More than 20 J/ψ decay channels, including $J/\psi \rightarrow \gamma K^+ K^- \pi^+ \pi^-$, $\gamma \pi^+ \pi^- \pi^+ \pi^-$, $K^*(892)^\pm K^\mp$, $K^*(892)^0 K_S$, and $\bar{K}^*(892)^0 K_S$ decays are generated using uniform phase space generators, and no peak is produced in the $K^+ \pi^-$ mass spectrum. This means that the low mass broad structure in the $K^+ \pi^-$ mass spectrum does not come from these background channels. From the Monte Carlo simulation, we also see that the background level in $J/\psi \rightarrow \bar{K}^*(892)^0 K^+ \pi^-$ is about 1/7 of that in $J/\psi \rightarrow K^+ K^- \pi^+ \pi^-$. Therefore, we think $J/\psi \rightarrow \bar{K}^*(892)^0 K^+ \pi^-$ is a good place to study the κ . The background level ranges from 10 to 15 % in this analysis.

We also study 58 million Monte Carlo $J/\psi \rightarrow anything$ events which are generated using the Lund-charm model [33]. The generator is developed for simulating J/ψ inclusive decay. In the models, charmonium decays into hadrons via quarks and gluons are simulated. Quarks and gluons shower development and their hadronization are handled by the LUND string model. The model reproduces the main properties of hadronic events from J/ψ inclusive decay. The process, $J/\psi \rightarrow K^*(892)\kappa$ is not included in the generator. Using the same selection criteria on this Monte Carlo sample as those for data, the scatter plot of $M_{K^+ \pi^-}$ versus $M_{K^- \pi^+}$ (Fig. 1b), shows no accumulation of events around the region where the $K^*(892)^0$ and $\bar{K}^*(892)^0$ bands cross. There is no corresponding broad low mass enhancement in the invariant mass spectrum of $K^+ \pi^-$ (or $K^- \pi^+$) recoiling against $\bar{K}^*(892)^0$ (or $K^*(892)^0$ for the charge conjugate channel) shown as the shaded area in Fig. 3b (or in the insertion of Fig. 3b), and there is no diagonal band of the low mass enhancement in the Dalitz plot of $J/\psi \rightarrow \bar{K}^*(892)^0 K^+ \pi^-$ (or $J/\psi \rightarrow K^*(892)^0 K^- \pi^+$). Because the generator of this Monte Carlo simulation does not contain the process $J/\psi \rightarrow K^*(892)\kappa$, the Monte Carlo shows different structures at lower $K\pi$ mass region from those of data. This difference just means that the low mass enhancement is not due to backgrounds coming from other J/ψ decay channels.

In the PWA of $J/\psi \rightarrow \bar{K}^*(892)^0 K^+ \pi^-$, the $\bar{K}^*(892)^0$ is treated as a stable particle. After integrating over the $K^- \pi^+$ angular information, no interference effect is expected between the charge conjugate processes, $J/\psi \rightarrow \bar{K}^*(892)^0 K^+ \pi^-$ and $K^*(892)^0 K^- \pi^+$, if the solid angle coverage of the detector is 4π . We examined the interference effect taking into account the detector acceptance and the width of the $\bar{K}^*(892)^0$ using Monte Carlo simulation and find that the interference effect in the cross region of the two $K^*(892)^0$ bands in the scatter plot is negligibly small, and that the interference between $\bar{K}^*(892)^0 K^+ \pi^-$ and $\rho K \bar{K}$ (or $K_J^*(1430) K \pi$) is also negligible. We ignore these interferences in the PWA analyses.

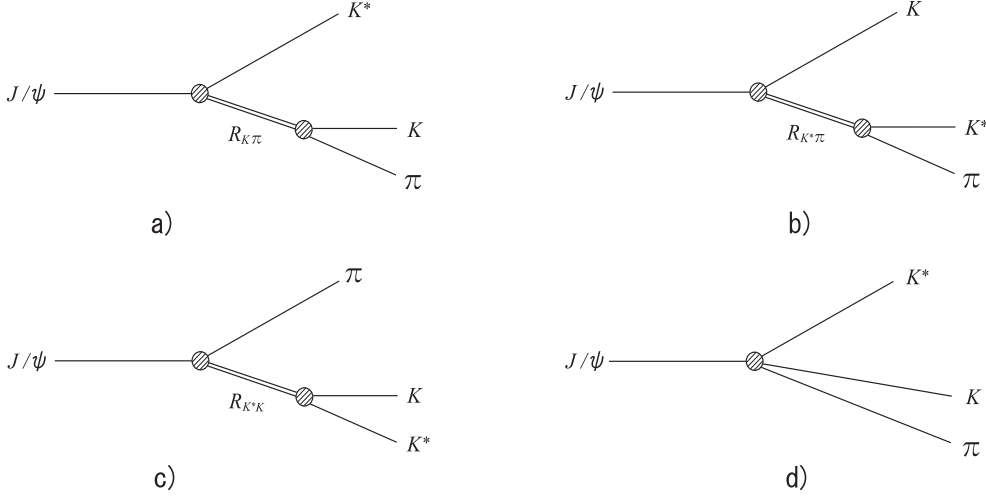


Fig. 4. Decay mechanisms for a) $J/\psi \rightarrow K^*(892)^0 R_{K\pi}$, b) $J/\psi \rightarrow K R_{K^*\pi}$, c) $J/\psi \rightarrow \pi R_{K^*K}$, and d) $J/\psi \rightarrow K^* K \pi$. $R_{K\pi}$, $R_{K^*\pi}$, and R_{K^*K} are intermediate resonant states decaying into $K\pi$, $K^*\pi$ and K^*K , respectively. K^* denotes $K^*(892)^0$.

We consider the $K^*(892)^0 K \pi$ channel in J/ψ decays, with well defined quantum states recoiling against the $K^*(892)^0$, is suitable to study the κ in the $K\pi$ system. The $K^*(892)^0 K \pi$ system simplifies the PWA, and backgrounds can be treated easily. To simplify the analysis, one of the charge conjugate states, $\bar{K}^*(892)^0 K^+ \pi^-$, is used, and it has enough events for this analysis. As mentioned above, the analysis of this channel is not affected by the charge conjugate state, $K^*(892)^0 K^- \pi^+$, since the interference between them is found to be negligibly small.

Four decay mechanisms considered in our analyses are shown in Fig. 4. These are $J/\psi \rightarrow K^* R_{K\pi}$ (Fig. 4a), $J/\psi \rightarrow K R_{K^*\pi}$ (Fig. 4b), $J/\psi \rightarrow \pi R_{K^*K}$ (Fig. 4c) and $J/\psi \rightarrow K^* K \pi$ (Fig. 4d), where $R_{K\pi}$, $R_{K^*\pi}$ and R_{K^*K} are intermediate resonant states decaying into $K\pi$ (κ , $K_0^*(1430)$, $K_2^*(1430)$, $K_2^*(1920)$), $K^*\pi$ ($K_1(1270)$, $K_1(1400)$) and K^*K ($b_1(1235)$), respectively. (Here, K^* denotes $K^*(892)^0$.) The independent PWA analyses by Method A and Method B have been performed on the $\bar{K}^*(892)^0 K^+ \pi^-$ channel. The same data set is used in both analyses.

Method A is based on the covariant helicity amplitude analysis [34]. The maximum likelihood method is utilized in the fit. The fit is performed by using Breit-Wigner parameterizations with an s -dependent width, $\rho(s)$, (See eq. (1) below.) for the low mass enhancement and with constant widths for the other intermediate states. Fits are also performed using two other parameterizations of constant width and of a width for the κ using a unitarization approach with chiral symmetry [16] as follows;

$$BW \propto 1/(M^2 - s - i\sqrt{s}\Gamma_\kappa(s)) , \Gamma_\kappa(s) = g_\kappa^2 \cdot k_K/8\pi s , \quad (1)$$

$$BW \propto 1/(M^2 - s - iM\Gamma_{const}) , \quad (2)$$

and

$$BW \propto 1/(M^2 - s - i\sqrt{s}\Gamma_\kappa(s)) , \Gamma_\kappa(s) = \alpha_\kappa k_K . \quad (3)$$

Eq. (1) is for Method A, eq. (2) is for Method A-1, and eq. (3) is for Method A-2.

The broad low mass enhancement is fit by a 0^+ resonance. The possibility that its spin-parity is 1^- , 2^+ , \dots is excluded by at least 10σ . If the kappa is removed from the fit, the log-likelihood becomes worse by 294. So, its statistical significance is above 20σ . This iso-spinor scalar resonance is considered to be the κ particle. The above parameterizations are tried for the κ . Though these parameterizations have different behavior, the quality of the fits given by them is almost the same. This is because there are many resonances with interferences between them, and changes in one can be compensated by changes in the others while keeping the total contribution unchanged. Though mass and width parameters given by these parameterizations are somewhat different, the shapes of the κ obtained by these parameterizations are similar, and the pole positions are close to each other.

The biggest peak at about $1430 \text{ MeV}/c^2$ in the $K^+\pi^-$ spectrum is relatively complex, containing 0^+ , 1^- , and 2^+ components. The 0^+ and 2^+ components are identified to be $K_0^*(1430)$ and $K_2^*(1430)$, respectively, and their masses and widths determined from the fit are consistent with PDG values [6]. A 1^- is included in the fit in this region. Changes by removing it are considered in the systematic uncertainties. In the higher $K^+\pi^-$ mass region, a broad resonance is needed. It is found that different treatments of it have little influence on the mass and width of the κ .

$K_1(1270)$ and $K_1(1400)$ are used to fit the enhancement near threshold of the $\bar{K}^*(892)^0\pi^-$ spectrum, and $b_1(1235)$ is used to improve the fit in the $\bar{K}^*(892)^0K^+$ spectrum. Because the mass of $b_1(1235)$ is below $\bar{K}^*(892)^0K$ threshold, only the tail of $b_1(1235)$ affects the fit of the $\bar{K}^*(892)^0K$ spectrum. Changes caused by removing the $b_1(1235)$ are included in the systematic uncertainties.

In the PWA, the backgrounds from the charge conjugate channel $J/\psi \rightarrow K^*(892)^0K^-\pi^+$ and from $J/\psi \rightarrow \bar{K}^*(892)^0K_S$ and $K_S \rightarrow \pi^+\pi^-$ where π^+ is misidentified with K^+ are fitted by non-interfering amplitudes, and the background from other J/ψ decay channels, including $J/\psi \rightarrow \rho K \bar{K}$ are fitted by non-interfering phase space. The uncertainty of the background level is considered, and its influence on the mass and width of the κ is estimated and

Table 1

Masses, widths and pole positions of the κ obtained by Methods A (eq. (1)), B (eq. (4)), A-1 (eq. (2)), and A-2 (eq. (3)). The mass and width values averaged for A and B are given. The first term errors are statistical ones and the second show systematic uncertainties estimated in the analyses.

	Mass (MeV/ c^2)	Width (MeV/ c^2)	Pole position (MeV/ c^2)
Method A	$874 \pm 25_{-55}^{+12}$	$518 \pm 65_{-87}^{+27}$	$(836 \pm 38_{-87}^{+18}) - i(329 \pm 66_{-46}^{+28})$
Method B	$896 \pm 54_{-44}^{+64}$	$463 \pm 88_{-31}^{+55}$	$(865 \pm 70_{-60}^{+78}) - i(271 \pm 67_{-23}^{+44})$
Average	$878 \pm 23_{-55}^{+64}$	$499 \pm 52_{-87}^{+55}$	$(841 \pm 30_{-73}^{+81}) - i(309 \pm 45_{-72}^{+48})$
Method A-1	$745 \pm 26_{-91}^{+14}$	$622 \pm 77_{-78}^{+61}$	$(799 \pm 37_{-90}^{+16}) - i(290 \pm 33_{-38}^{+25})$
Method A-2	$1140 \pm 39_{-80}^{+47}$	$1370 \pm 156_{-148}^{+406}$	$(811 \pm 74_{-83}^{+17}) - i(285 \pm 20_{-42}^{+18})$

is put into the systematic errors.

Since there exist broad $K^+\pi^-$ resonances around 1430 MeV and those broad resonances and other background processes $K^*(892)$, K_S , and PS contribute in the κ region, and because of the complicated interferences between κ and other resonances, different solutions are obtained in the fits. These solutions give almost the same fit quality and almost the same pole position of κ . Uncertainties coming from the multi-solutions on the κ parameters are included in the systematic errors.

The fit obtained in the analysis is shown by the solid histogram in Fig. 5a for the $K^+\pi^-$ invariant mass spectrum. The data are shown by crosses with error bars. The contribution of the κ is shown by the dark shaded histogram. The fit of the $\bar{K}^*(892)^0\pi^-$ invariant mass spectrum is shown by the solid histogram in Fig. 5c. The fit for the angular distribution of the whole $K^+\pi^-$ mass region is shown by the solid histogram in Fig. 5e, and that for the angular distribution of the $K^+\pi^-$ mass below 1.0 GeV/ c^2 is shown by the histogram in Fig. 5g.

The values for Breit-Wigner parameters of mass and width and those for the pole position for the κ obtained in Method A are given in Table 1. Systematic uncertainties in the mass and width of the κ include the changes from 1σ variations of the masses and widths of the other resonances, different treatments of background, and uncertainties from the fitting.

Mass and width parameters of intermediate resonances and of those background processes in the fit of Method A are tabulated in Table 2. Errors shown in the table are only statistical.

Method B uses the VMW (Variant Mass and Width) method, a covariant field theoretical approach consistent with generalized unitarity [24]. In this method, the total amplitude is expressed as a coherent sum of respective amplitudes, corresponding to the relevant processes of strong interactions among all color-

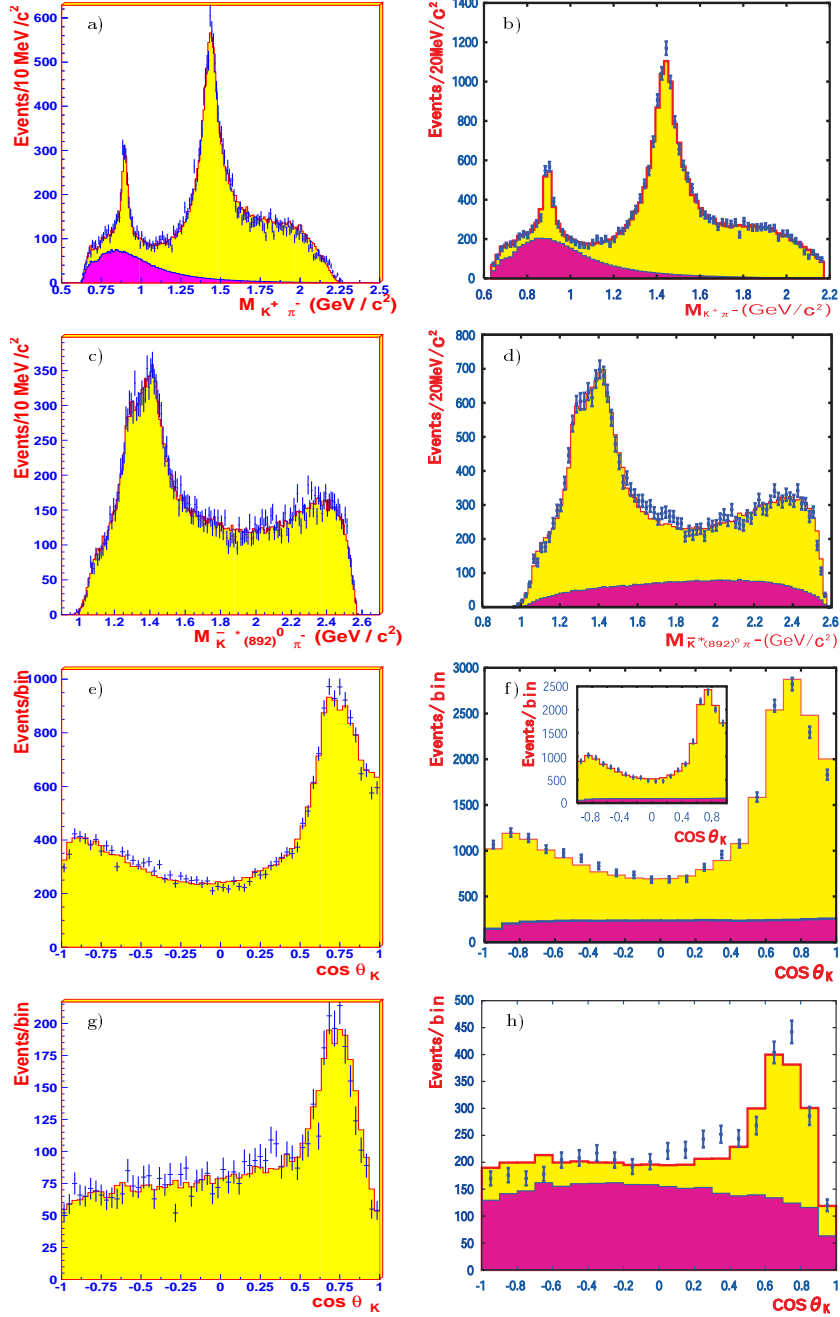


Fig. 5. Analysis results by Method A. a) The $K^+\pi^-$ invariant mass spectrum. c) The $\bar{K}^*(892)^0\pi^-$ invariant mass spectrum. e) The K^+ angular distribution in the $K^+\pi^-$ center of mass system for the whole $K^+\pi^-$ mass region, and g) that for the $K^+\pi^-$ mass region below $1.0 \text{ GeV}/c^2$. Crosses with error bars are data. Solid histograms show fit results, and the dark shaded histogram in a) is the contribution from the κ . Analysis results by Method B. b) The $K^+\pi^-$ invariant mass spectrum. d) The $\bar{K}^*(892)^0\pi^-$ invariant mass spectrum. f) The K^+ angular distribution in the $K^+\pi^-$ center of mass system for the whole $K^+\pi^-$ mass region with that for above $1.0 \text{ GeV}/c^2$ in the insertion, and h) that for the $K^+\pi^-$ mass region below $1.0 \text{ GeV}/c^2$. Crosses with error bars are data. Solid histograms are fit, and dark shaded histograms are contributions from the κ .

Table 2

Mass and Width values of intermediate resonance states and those of background processes in the fits of Method A and Method B. BG and PS denotes background and phase space, respectively.

Resonances	Method A		Method B	
	mass (MeV/ c^2)	Γ (MeV/ c^2)	mass (MeV/ c^2)	Γ (MeV/ c^2)
$\kappa \rightarrow K\pi$	874 \pm 25	518 \pm 65	896 \pm 54	463 \pm 88
$K_0^*(1430) \rightarrow K\pi$	1436 \pm 46	348 \pm 55	1448 \pm 37	200 ¹⁾
$K_2^*(1430) \rightarrow K\pi$	1434 \pm 7	101 \pm 15	1443 \pm 48	97 \pm 16
X(1430) (1^-) $\rightarrow K\pi$	1426 \pm 6	152 \pm 16	not included ²⁾	
$K_2^*(1920) \rightarrow K\pi$	1914 \pm 36	590 \pm 110	1911 \pm 24	244 \pm 95
$K_1(1270) \rightarrow K^*(892)\pi$	1279 \pm 10	131 \pm 21	1271 \pm 12	104 \pm 33
$K_1(1400) \rightarrow K^*(892)\pi$	1418 \pm 8	152 \pm 16	1429 \pm 31	200 ³⁾
$b_1(1235) \rightarrow K^*(892)K$	fixed ⁴⁾	fixed ⁴⁾	fixed ⁴⁾	fixed ⁴⁾
Direct $\bar{K}^*(892)^0 K\pi$	not included ²⁾		included ⁵⁾	
$K^*(892)$ BG $\rightarrow K\pi$	fixed ⁴⁾	fixed ⁴⁾	fixed ⁴⁾	fixed ⁴⁾
$K^*(1410)$ BG $\rightarrow K\pi$	not included ²⁾		fixed ⁴⁾	fixed ⁴⁾
K_S BG	715 ⁶⁾	46 ⁶⁾	715 ⁶⁾	46 ⁶⁾
$K^*(892)K\pi$ PS BG	included ⁵⁾		included ⁵⁾	

1) Bound for the lower limit which is set to be consistent with that of the PDG tables.

2) The process is not included in the fit.

3) Bound for the upper limit which is set to be consistent with that of the PDG tables.

4) The value is fixed to that of the PDG tables.

5) The process is included in the fit.

6) The value is parameterized by the Monte Carlo simulation and fixed in the fit.

singlet hadrons. As the bases of the S -matrix for the strong interaction, a residual interaction of QCD, all unstable (or resonant) as well as stable hadrons which are to be color-singlet bound states of quarks, anti-quarks and gluons are to be included. The propagator of a resonant particle is given by the conventional Feynman propagator with substitution of $i\epsilon$ by $i\sqrt{s}\Gamma(s)$.

For the scalar $K\pi$ -resonant particles, $R_{K\pi}$'s are the κ and $K_0^*(1430)$. The Lagrangian of strong interaction, \mathcal{L}_S , describing the process in Fig. 4a is taken to be the most simple form. This form and the corresponding decay amplitude \mathcal{F}_S are given by

$$\begin{aligned}
\mathcal{L}_S &= \sum_{R=\kappa, K_0^*} (\xi_R \psi_\mu K_\mu^* R + g_R R K \pi), \\
\mathcal{F}_S &= S_{h_\psi h_{K^*}} \sum_{R=\kappa, K_0^*} r_R e^{i\theta_R} \Delta_R(s_{K\pi}), \\
\Delta_R(s_{K\pi}) &= \frac{m_R \Gamma_R}{m_R^2 - s_{K\pi} - i\sqrt{s_{K\pi}} \Gamma_R(s_{K\pi})}, \tag{4}
\end{aligned}$$

where $\Delta_R(s_{K\pi})$ is the Breit-Wigner formula with $\Gamma_R(s_{K\pi}) = pg_R^2/(8\pi s_{K\pi})$, describing the decay of $R = \kappa$ and $K_0^*(1430)$, and $S_{h_\psi h_{K^*}}$ is the helicity amplitude $S_{h_\psi h_{K^*}} \equiv \epsilon_\mu^{(h_\psi)} \tilde{\epsilon}_\mu^{(h_{K^*})}$. $S_{h_\psi h_{K^*}} r_R e^{i\theta_R}$ describes the S -matrix element ${}_{out}\langle RK^* | J/\psi \rangle_{in}$, where $e^{i\theta_R}$ parametrizes the rescattering phase of ${}_{out}\langle RK^* |$. This form of \mathcal{F}_S is consistent with the generalized unitarity of the S -matrix.

The decay amplitudes through the tensor $R_{K\pi}$, $R_{K^*\pi}$, and R_{K^*K} , denoted as \mathcal{F}_D , \mathcal{F}_{K_1} , and \mathcal{F}_{b_1} , respectively, are obtained in a similar manner. The direct $K\pi$ production amplitude is taken to be $\mathcal{F}_{dir} = S_{h_\psi h_{K^*}} r_{K\pi} e^{i\theta_{K\pi}}$, which is from $\mathcal{L}_{dir} \sim \xi_{K\pi} \psi_\mu K_\mu^* K\pi$. The total amplitude \mathcal{F} is given by the sum of all these amplitudes,

$$\mathcal{F} = \mathcal{F}_S + \mathcal{F}_D + \mathcal{F}_{K_1} + \mathcal{F}_{b_1} + \mathcal{F}_{dir}. \tag{5}$$

We also consider the background processes coming from $J^P = 1^- K^*(892)$ and $K^*(1410)$ (decaying into $K^+\pi^-$), from K_S , and from phase space $K^*(892)K\pi$, which are described by the amplitudes incoherent with the above \mathcal{F} . The details are described elsewhere [30]. The treatments of resonances and background processes in this method are the same as those in Method A, except for the $K^*(1410)\bar{K}^*(892)$ and $K^*(892)K\pi$ processes, as explained below.

The least χ^2 method is used for the fitting of the mass distribution of $K^+\pi^-$, that of $\bar{K}^*(892)^0\pi^-$, and the K^+ angular distribution in the $K^+\pi^-$ system. The results obtained in this analysis are shown by the solid histograms for the $K^+\pi^-$ invariant mass spectrum in Fig. 5b and for the $\bar{K}^*(892)^0\pi^-$ mass spectrum in Fig. 5d. The data for the analysis are shown by crosses with error bars. The contributions of the κ are shown by the dark shaded histograms superimposed on Figs. 5b and 5d. The results for the K^+ angular distributions in the whole $K^+\pi^-$ mass region and below 1.0 GeV/ c^2 are shown by the solid histograms in Figs. 5f and 5h, respectively, and that for the mass region above 1.0 GeV/ c^2 is inserted in Fig. 5f. The contributions of the κ are also shown by the dark shaded histograms in the figures.

The values for Breit-Wigner parameters of mass and width and pole position for the κ obtained in the analysis of Method B are given in Table 1. Uncertainties are estimated on the same items as in Method A. Method B takes the direct $\bar{K}^*(892)^0 K^+\pi^-$ process to be coherent and phase space background contribution to be incoherent. The contribution of the latter is estimated us-

ing the results obtained in Method A. The uncertainties of it are included in the systematic errors of the κ parameters. The $\bar{K}^*(892)^0 K^*(1410)$ amplitude is taken as an incoherent background process. The $K^*(892)^0$ events are considered to be associated with $K^-\pi^+$ and/or $\bar{\kappa}$ which are in the $\bar{K}^*(892)^0$ region. No interference is expected between charge conjugate states. A coherent $\bar{K}^*(892)^0 K^*(1410)$ amplitude is also examined, and the difference is also included in the uncertainty for the κ parameters. Uncertainties for the κ parameters contain also the change from 1σ variations of the masses and widths of the other resonances and uncertainties of the fit. Mass and width parameters of intermediate resonances and of background processes in the fit by Method B are also tabulated in Table 2. Errors shown in the table are only statistical.

The $\chi^2/\text{d.o.f}$ value is 1.10. We examined also the fit without the κ resonance and obtained the value to be 2.83. In the latter, the parameters for the K_S background are fixed.

The results obtained in the two analyses reproduce the data well and are in good agreement with each other. Both fits favor strongly that the low mass enhancement of the $K^+\pi^-$ system is a resonance. The scalar resonance is considered to be the κ which is necessary in both fits. The average values for Breit-Wigner parameters of masses and widths for the κ (given in the third row in Table 1) are obtained from Methods A and B,

$$M_\kappa = 878 \pm 23_{-55}^{+64} \text{ MeV}/c^2, \quad \Gamma_\kappa = 499 \pm 52_{-87}^{+55} \text{ MeV}/c^2,$$

where the first term errors are statistical ones. The second ones show total uncertainties, taking the largest values between systematic uncertainties of Methods A and B. The average values are in good agreement with those obtained in the analysis of $K\pi$ scattering phase shifts [11]. The κ parameters obtained are also consistent with those obtained in the analysis of $D^+ \rightarrow K^-\pi^+\pi^+$ in the E791 experiment [25] with $M_\kappa = 797 \pm 19 \pm 43 \text{ MeV}/c^2$ and $\Gamma_\kappa = 410 \pm 43 \pm 87 \text{ MeV}/c^2$. The relative contribution for the kappa normalized for the total event number ranges between 0.08 and 0.25 taking the effects coming from the multi-solutions and systematic uncertainties in the analyses into account.

Recent analyses [35] of $J/\psi \rightarrow 1^-0^-$ decays and 0^-0^- decays show the large amount of strong phases between relevant amplitudes. This fact suggests that, in the relevant $J/\psi \rightarrow K^*(892)K\pi$ decay, the $K\pi$ system is not isolated out of the final three-body system, and accordingly in the decay amplitude the phase of the pure $K\pi$ -scattering amplitude is not directly observed experimentally.

In Methods A and B, the phase of the total $J/\psi \rightarrow K^*(892)K\pi$ amplitude comes from a sum of respective contributions of the S -matrix elements with the final systems, $K^*(892)\kappa$, $K^*(892)K_0^*(1430)$, $K^*(892)K\pi$, etc. We obtained

the κ resonance with width, $\Gamma_\kappa \simeq 500\text{MeV}/c^2$ in the Breit-Wigner parameterization, which is consistent with the generalized unitarity of S-matrix. This behavior is also consistent with the result of analysis of $D^+ \rightarrow K^-\pi^+\pi^+$ process in the E791 experiment [25].

In conclusion, we have shown that the low mass enhancement in the invariant mass spectrum of $K^+\pi^-$ in the $J/\psi \rightarrow \bar{K}^*(892)^0 K^+\pi^-$ decays comes neither from phase space, nor from other J/ψ decay processes. The angular distribution of K in the $K\pi$ rest frame in the low mass region shows S-wave decay. Two independent analyses for the process, by the covariant helicity amplitude method and by the VMW method, have been performed, providing a cross check with each other. They reproduce the data well, and the results are in good agreement. The low mass enhancement is well described by the scalar resonance κ , which is highly required in the analyses. Parameter values for BW mass and width of the κ , averaged from those obtained by these two methods, are $878 \pm 23_{-55}^{+64} \text{MeV}/c^2$ and $499 \pm 52_{-87}^{+55} \text{MeV}/c^2$, respectively. They are in good agreement with those obtained in the analysis on the $K\pi$ scattering phase shifts. The pole position is determined to be $(841 \pm 30_{-73}^{+81}) - i(309 \pm 45_{-72}^{+48}) \text{MeV}/c^2$ from the average values.

Acknowledgements

The BES collaboration thanks the staff of BEPC for their hard efforts. This work is supported in part by the National Natural Science Foundation of China under contracts Nos. 10491300, 10225524, 10225525, 10425523, the Chinese Academy of Sciences under contract No. KJ 95T-03, the 100 Talents Program of CAS under Contract Nos. U-11, U-24, U-25, and the Knowledge Innovation Project of CAS under Contract Nos. U-602, U-34 (IHEP), the National Natural Science Foundation of China under Contract No. 10225522 (Tsinghua University), the Department of Energy under Contract No. DE-FG02-04ER41291 (U Hawaii), the Core University Program of Japan Society for the Promotion of Science, JSPS under Contract No. JR-02-B4, the fund for the international collaboration and exchange of RIQS, Nihon-U.

References

- [1] N. A. Törnqvist, Proc. Workshop at Yukawa Institute, Kyoto, June 12-14, 2000, KEK Proceedings 2000-4, ed. S. Ishida et al., p.224, and related articles in the Proceedings.
- [2] N. Wu (BES Collaboration), ‘BES R measurements and J/ψ Decays’, Proc.

of the XXXVIth Recontres de Moriond, Les Arcs, France, March 17-24, 2001, ed. J. Tran Thanh Van. 2001 QCD and High Energy Hadronic Interactions, p.3.

- [3] E. M. Aitala et al. (Fermilab E791 Collaboration), Phys. Rev. Lett. **86** (2001) 770.
- [4] J. Z. Bai et al. (BES Collaboration), High Energy Phys. Nucl. Phys. **28** (2004) 215.
- [5] M. Ablikim et al. (BES Collaboration), Phys. Lett. **B598** (2004) 149.
- [6] S. Eidelman et al., Phys. Lett. **B592** (2004) 1.
- [7] R. Delbourgo and M. D. Scadron, Phys. Rev. Lett. **48** (1982) 379.
- [8] M. Ishida, Prog. Theor. Phys. **101** (1999) 661.
- [9] E. van Beveren et al., Z. Phys. **C30** (1986) 651.
- [10] D. Aston et al., Nucl. Phys. **B296** (1988) 253.
- [11] S. Ishida et al., Prog. Theor. Phys. **98** (1997) 621.
- [12] D. Black et al., Phys. Rev. **D58** (1998) 054012.
- [13] J. A. Oller and E. Oset, Phys. Rev. **D60** (1999) 074023.
- [14] M. J. Jamin et al., Nucl. Phys. **B587** (2000) 331.
- [15] D. Bugg, Phys. Lett. **B572** (2003) 1.
- [16] H. Q. Zheng et al., Nucl. Phys. **A733** (2004) 235.
- [17] D. Lohs, Phys. Lett. **B234** (1990) 235.
- [18] N. A. Törnqvist, Z. Phys. **C68** (1995) 647.
- [19] A. V. Anisovich and A. V. Sarantsev, Phys. Lett. **B413** (1997) 137.
- [20] S. N. Cherry and M. R. Pennington, Nucl. Phys. **A688** (2001) 823.
- [21] S. Ishida et al., Prog. Theor. Phys. **95** (1996) 747; **98** (1997) 1005.
- [22] For a comment and discussions on σ , see M. R. Pennington, Proc. Workshop on Hadron Spectroscopy, Frascati, March, 1999, ed. by T. Bressani et al., Frascati Series, vol. 15, 1999, p.95; S. Ishida, *ibid.* p.85; M. Ishida, *ibid.* p.115.
- [23] M. Ishida, Prog. Theor. Phys. **96** (1996) 853; Proc. of WHS99, Frascati, Frascati Physics series 15 (1999), hep-ph/9905261.
- [24] S. Ishida et al., Prog. Theor. Phys. **95** (1996) 745; M. Ishida et al., Proc. of Int. Symposium on Hadron Spectroscopy, Chiral Symmetry and Relativistic Description of Bound Systems, Tokyo, February 24-26, 2003, KEK Proceeding 2003-7, 2003, p143; M. Ishida et al., Proc. of Int. Workshop on Hadron Spectroscopy and Search for Chiral Particles in J/ψ Decay Data at BES, KEK, Feb. 28 - Mar. 1, 2003, KEK Proceeding 2003-10, 2003, p.34.

- [25] E. M. Aitala et al. (Fermilab E791 Collaboration), Phys. Rev. Lett. **89** (2002) 121801.
- [26] J. Z. Bai et al. (BES Collaboration), hep-ex/0304001.
- [27] J. M. Link et al., Phys. Lett. **B535** (2002) 430.
- [28] S. Anderson et al., Phys. Rev. **D63** (2001) 090001.
- [29] N. Wu, Proc. of Int. Symposium on Hadron Spectroscopy, Chiral Symmetry and Relativistic Description of Bound Systems, Tokyo, February 24-26, 2003, KEK Proceeding 2003-7, 2003, p.127.
- [30] T. Komada, Proc. of Int. Symposium on Hadron Spectroscopy, Chiral Symmetry and Relativistic Description of Bound Systems, Tokyo, February 24-26, 2003, KEK Proceeding 2003-7, 2003, p.135; Proc. of 10th Hadron Spectroscopy Conference, Aschaffenburg, Germany, 31 Aug. - 6 Sep. 2003, AIP Conf. Proc. **717** (2004) 337.
- [31] W. G. Li, Proc. of 10th Hadron Spectroscopy Conference, Aschaffenburg, Germany, 31 Aug. - 6 Sep. 2003, AIP Conf. Proc. **717** (2004) 495.
- [32] J. Z. Bai et al., Nucl. Instr. Meth. **A344** (1994) 319; J.Z. Bai et al., Nucl Instr. Meth. **A458** (2001) 627.
- [33] J. C. Chen et al., Phys. Rev. **D62** (2000) 034003.
- [34] N. Wu and T. N. Ruan, Commun. Theor. Phys. (Beijing, China) **35** (2001) 547; **35** (2001) 693; **37** (2002) 309.
- [35] M. Suzuki, Phys. Rev. **D57** (1998) 5717; Phys. Rev. **D60** (1999) 051501.